2011

First Kepler results on compact pulsators - VI. Targets in the final half of the survey phase

R. H. Østensen

Rl Silvotti

S. Charpinet

R. Oreiro

S. Bloemen

See next page for additional authors

Recommended Citation

Østensen, Roy H., Roberto Silvotti, S. Charpinet, R. Oreiro, Steven Bloemen, A. S. Baran, M. D. Reed et al. "First Kepler results on compact pulsators–VI. Targets in the final half of the survey phase." Monthly Notices of the Royal Astronomical Society 414, no. 4 (2011): 2860-2870.

Monthly Notices
of the
ROYAL ASTRONOMICAL SOCIETY

Mon. Not. R. Astron. Soc. **414,** 2860–2870 (2011) doi:10.1111/j.1365-2966.2011.18405.x

First *Kepler* results on compact pulsators – VI. Targets in the final half of the survey phase

R. H. Østensen,[1⋆] R. Silvotti,[2] S. Charpinet,[3] R. Oreiro,[1,4] S. Bloemen,[1] A. S. Baran,[5,6] M. D. Reed,[7] S. D. Kawaler,[6] J. H. Telting,[8] E. M. Green,[9] S. J. O'Toole,[10] C. Aerts,[1,11] B. T. Gänsicke,[12] T. R. Marsh,[12] E. Breedt,[12] U. Heber,[13] D. Koester,[14] A. C. Quint,[6] D. W. Kurtz,[15] C. Rodríguez-López,[16,17] M. Vučković,[1,18] T. A. Ottosen,[8,19] S. Frimann,[8,19] A. Somero,[8,20] P. A. Wilson,[8,21] A. O. Thygesen,[8] J. E. Lindberg,[8,22] H. Kjeldsen,[19] J. Christensen-Dalsgaard,[19] C. Allen,[23] S. McCauliff[23] and C. K. Middour[23]

[1] *Instituut voor Sterrenkunde, K. U. Leuven, Celestijnenlaan 200D, 3001 Leuven, Belgium*
[2] *INAF-Osservatorio Astronomico di Torino, Strada dell'Osservatorio 20, 10025 Pino Torinese, Italy*
[3] *Laboratoire d'Astrophysique de Toulouse-Tarbes, Université de Toulouse, 14 Av. Edouard Belin, Toulouse 31400, France*
[4] *Instituto de Astrofísica de Andalucía, Glorieta de la Astronomía s/n, 18008 Granada, Spain*
[5] *Mt. Suhora Observatory, Cracow Pedagogical University, Podchorazych 2, 30-084 Krakow, Poland*
[6] *Department of Physics and Astronomy, Iowa State University, Ames, IA 50011, USA*
[7] *Department of Physics, Astronomy, and Materials Science, Missouri State University, Springfield, MO 65804, USA*
[8] *Nordic Optical Telescope, 38700 Santa Cruz de La Palma, Spain*
[9] *Steward Observatory, University of Arizona, 933 N. Cherry Ave., Tucson, AZ 85721, USA*
[10] *Australian Astronomical Observatory, PO Box 296, Epping, NSW 1710, Australia*
[11] *Department of Astrophysics, IMAPP, Radboud University Nijmegen, 6500 GL Nijmegen, the Netherlands*
[12] *Department of Physics, University of Warwick, Coventry CV4 7AL*
[13] *Dr. Karl Remeis-Observatory & ECAP, Astronomical Institute, FAU Erlangen-Nuremberg, Sternwartstr. 7, 96049 Bamberg, Germany*
[14] *Institut für Theoretische Physik und Astrophysik, Universität Kiel, 24098 Kiel, Germany*
[15] *Jeremiah Horrocks Institute of Astrophysics, University of Central Lancashire, Preston PR1 2HE*
[16] *Departamento de Física Aplicada, Universidade de Vigo, Campus Lagoas-Marcosende s/n, 36310 Vigo, Spain*
[17] *Department of Physics and Astronomy, University of Delaware, 217 Sharp Lab, Newark, DE 19716, USA*
[18] *European Southern Observatory, Alonso de Córdova 3107, Vitacura, Casilla, 19001 Santiago, Chile*
[19] *Department of Physics and Astronomy, Aarhus University, 8000 Aarhus C, Denmark*
[20] *Tuorla Observatory, Department of Physics and Astronomy, University of Turku, Väisäläntie 20, FI-21500 Piikkiö, Finland*
[21] *Astrophysics Group, School of Physics, University of Exeter, Stocker Road, Exeter EX4 4QL*
[22] *Centre for Star and Planet Formation, Natural History Museum of Denmark, University of Copenhagen, Ø. Voldgade 5-7, Copenhagen DK-1350, Denmark*
[23] *Orbital Sciences Corporation/NASA Ames Research Center, Moffett Field, CA 94035, USA*

Accepted 2011 January 21. Received 2011 January 20; in original form 2010 December 18

ABSTRACT

We present results from the final 6 months of a survey to search for pulsations in white dwarfs (WDs) and hot subdwarf stars with the *Kepler* spacecraft. Spectroscopic observations are used to separate the objects into accurate classes, and we explore the physical parameters of the subdwarf B (sdB) stars and white dwarfs in the sample. From the *Kepler* photometry and our spectroscopic data, we find that the sample contains five new pulsators of the V1093 Her type, one AM CVn type cataclysmic variable and a number of other binary systems.

This completes the survey for compact pulsators with *Kepler*. No V361 Hya type of short-period pulsating sdB stars were found in this half, leaving us with a total of one single multiperiodic V361 Hya and 13 V1093 Her pulsators for the full survey. Except for the sdB pulsators, no other clearly pulsating hot subdwarfs or white dwarfs were found, although a few

⋆E-mail: roy@ster.kuleuven.be

low-amplitude candidates still remain. The most interesting targets discovered in this survey will be observed throughout the remainder of the *Kepler* mission, providing the most long-term photometric data sets ever made on such compact, evolved stars. Asteroseismic investigations of these data sets will be invaluable in revealing the interior structure of these stars and will boost our understanding of their evolutionary history.

Key words: surveys – binaries: close – stars: oscillations – subdwarfs – white dwarfs.

1 INTRODUCTION

The *Kepler* spacecraft was launched in 2009 March, with the primary aim to find Earth-size planets within the habitable zone around solar-like stars using the transit method (Borucki et al. 2010). In order to have a high probability of finding such planets, the spacecraft continuously monitors the brightness of ∼100 000 stars with close to micromagnitude precision. As a byproduct of the planet hunt, high-quality photometric data of variable stars are obtained, an incredibly valuable input for the study of binary stars (Prsa et al. 2011) and asteroseismology (Gilliland et al. 2010a).

The first four quarters of the *Kepler* mission were dedicated to a survey phase, and a substantial number of target slots for short-cadence (SC) observations were made available to the Kepler Asteroseismic Science Consortium: 512 slots in the initial roll position (Q1) and 140 in the following quarters. The series of papers of which this is the sixth deals with the search for compact pulsators,[1] and the results from the first half of the survey are described in Østensen et al. (2010b, Paper I). Kawaler et al. (2010a, Paper II) describe KIC 10139564, a short-period subdwarf B (sdB) pulsator (V361 Hya star). Five long-period sdB pulsators (V1093 Her stars) are described in Reed et al. (2010, Paper III), and one of them, KPD 1943+4058, is given a detailed asteroseismic analysis in Van Grootel et al. (2010, Paper IV). An asteroseismic analysis on another of the stars in Paper III, KIC 2697388, is given by Charpinet et al. (2011). Two more V1093 Her pulsators that appear to be in short-period binary systems with M-dwarf (dM) companions are described in Kawaler et al. (2010b, Paper V).

The first half of the survey also revealed that the eclipsing sdB+dM binary, 2M1938+4603 (KIC 9472174), is a low-amplitude pulsator with an exceptionally rich frequency spectrum (Østensen et al. 2010a), and the sdB+ WD binary, KPD 1946+4340 (KIC 7975824), was found to show eclipses, ellipsoidal modulation and Doppler beaming effects (Bloemen et al. 2011). This paper describes the content of the compact pulsator sample observed in the second half of the survey phase.

The *Kepler* field of view covers 105 deg^2 and is being observed in a broad bandpass (4200–9000 Å) using 42 CCDs mounted in pairs on 21 modules. Although the *Kepler* photometer samples the field every 6.54 s, telemetry restrictions do not permit the imaging data to be downloaded. Instead, pixel masks of targets deemed to be of interest must be uploaded to the spacecraft, and these pixels are averaged into samples of either approximately 1 minute for SC or half an hour for long cadence (LC).

The primary goal of the asteroseismology survey phase is therefore to identify the most interesting pulsators in the sample, so that these objects can then be followed throughout the remaining years of the mission. The primary goals for the compact pulsator survey were set out in Paper I, and for the sdB pulsators a substantial list of targets for further study was identified. However, no clearly pulsating WD was found in the first part of the sample, and it was hoped that the second part would bring more luck. This did not happen, so we are still without any confirmed WD pulsators to follow for the specific target part of the *Kepler* mission. Analyses of the five unambiguous V1093 Her pulsators found in this second half of the survey are presented by Baran et al. (2011, Paper VII). A study of the period spacings observed in many of the V1093 Her stars from the survey has been given by Reed et al. (2011, Paper VIII).

For an introduction to the pulsating sdB stars, we refer the reader to the earlier papers in this series. In this paper, we will provide photometric variability limits on all the stars from the second half of the sample and physical parameters for the hot subdwarf stars, as we did in Paper I. Moreover, we will also provide physical data from our spectroscopy on the WD stars.

We will also present analysis of the *Kepler* photometry for a number of objects that display long-period variability features, and for many of these we conclude that they are most likely to be binary systems composed of a hot subdwarf and a WD or a main-sequence star.

2 SURVEY SAMPLE

The methods used to select the sample stars were described in detail in Paper I. In brief, three groups submitted targets based on six different selection methods, which we designate a–f in Table 1. Only two stars in the current half of the sample were already classified as compact stars from earlier surveys (sample a), FBS 1907+425 and FBS 1903+432 (Abrahamian et al. 1990). The first one of these also appears in the Two-Micron All-Sky Survey (2MASS) colour-selected sample (b), but was dropped as a candidate after follow-up spectroscopy demonstrated that the star was a normal B star. It did, however, re-enter the survey sample through the Kepler Input Catalog (KIC) colour-selected sample (f). Eight stars appear in the SEGUE extension (Yanny et al. 2009) of the Sloan Digital Sky Survey (SDSS; Stoughton et al. 2002) (c), and all these are compact objects. 17 of the stars were selected based on UV excess from *Galex* satellite data (Martin et al. 2005) (d), and these are also all hot subdwarfs or WDs. Seven stars were chosen based on their position in the reduced proper motion (RPM) diagram (e), but only five of these turned out to be compact objects. As many as 22 stars were selected based only on KIC *gri* colours (f), and of these, 14 were not included in any of the other samples. Of the latter, nine were compact stars and five normal B–F stars. In total, four B and four F stars contaminate our sample of 47 targets and will not be discussed further here. The remaining compact pulsator candidates have been spectroscopically classified as WDs or WD composites (six objects), and hot subdwarfs or

[1] The term 'compact pulsators' is used to encompass all the various groups of pulsating white dwarfs and hot subdwarf stars.

Table 1. Compact pulsator candidates observed with *Kepler* in Q3 and Q4.

KIC	Name	Run	RA(J2000)	Dec.(J2000)	*Kp*	$F_{\rm cont}$	Sample	Class
2020175	J19308+3728	Q3.1	19:30:48.5	+37:28:19	15.49	0.722	ce†	sdB
2303576	J19263+3738	Q3.3	19:26:18.9	+37:38:15	17.45	0.928	c	He-sdO
2304943	J19275+3738	Q3.3	19:27:33.8	+37:38:55	16.18	0.692	c	sdB
2850093	J19237+3801	Q3.2	19:23:47.2	+38:01:44	14.73	0.298	f	F
3343613	J19272+3827	Q3.2	19:27:15.0	+38:27:19	15.74	0.469	df	He-sdOB
3353239	J19367+3825	Q4.1	19:36:46.3	+38:25:27	15.15	0.099	f	sdB
3527028	J19024+3840	Q4.2	19:02:25.7	+38:40:20	17.09	0.465	c	sdB
3938195	J19048+3903	Q4.1	19:04:49.5	+39:03:16	15.30	0.908	f	F
4547333	J19082+3940	Q3.3	19:08:17.1	+39:40:36	16.32	0.253	c‡	AM CVn
5340370	J18535+4035	Q4.2	18:53:31.1	+40:35:19	17.08	0.128	c	sdB
5557961	J19514+4043	Q4.3	19:51:26.2	+40:43:36	15.82	0.647	f	F
5769827	J18547+4105	Q4.1	18:54:45.0	+41:05:15	16.62	0.952	c	DA0
5938349	J18521+4115	Q3.2	18:52:10.1	+41:15:15	16.05	0.079	c	sdB
6371916	J19370+4145	Q3.3	19:37:01.1	+41:45:39	14.97	0.361	e	B
6522967	J19279+4159	Q3.2	19:27:58.7	+41:59:03	16.91	0.622	d	sdB
6614501	J19368+4201	Q3.3	19:36:50.0	+42:01:44	16.09	0.600	f	sdB
6878288	J19436+4220	Q3.1	19:43:37.0	+42:20:58	16.67	0.686	f	He-sdOB
7104168	FBS 1907+425	Q3.1	19:08:45.7	+42:38:32	15.48	0.189	af	sdB
7129927	J19409+4240	Q3.1	19:40:59.4	+42:40:31	16.59	0.585	e†	DA+DA
7335517	J18431+4259	Q3.2	18:43:06.7	+42:59:18	15.75	0.295	df	sdO+dM
7668647	FBS 1903+432	Q3.1	19:05:06.2	+43:18:31	15.40	0.226	af	sdBV
7799884	J18456+4335	Q4.1	18:45:37.2	+43:35:25	16.87	0.109	d	sdB
8054179	J19569+4350	Q3.1	19:56:55.6	+43:50:17	14.43	0.093	f	He-sdOB
8302197	J19310+4413	Q3.3	19:31:03.4	+44:13:26	16.43	0.256	f	sdBV
8874184	J19084+4508	Q4.1	19:08:24.7	+45:08:32	16.52	0.091	d	sdB
9095594	J19369+4526	Q3.2	19:36:59.4	+45:26:27	17.69	0.434	d	sdB
9211123	J19144+4539	Q3.3	19:14:27.7	+45:39:10	16.10	0.447	d	sdB
9637292	J19030+4619	Q3.1	19:03:02.0	+46:19:55	16.68	0.513	f	B
10001893	J19095+4659	Q3.2	19:09:33.5	+46:59:04	15.85	0.710	df	sdBV
10149211	J19393+4708	Q4.2	19:39:18.3	+47:08:55	15.52	0.240	f	sdB
10198116	J19099+4717	Q4.1	19:09:59.4	+47:17:10	16.41	0.238	de	DA
10207025	J19260+4716	Q3.3	19:26:05.9	+47:16:31	15.04	0.068	f	He-sdO
10449976	J18472+4741	Q3.2	18:47:14.1	+47:41:47	14.86	0.006	df	He-sdOB
10462707	J19144+4737	Q4.1	19:14:29.1	+47:37:41	16.89	0.072	d	sdB
10553698	J19531+4743	Q4.1	19:53:08.4	+47:43:00	15.13	0.385	f	sdB
10579536	J18465+4751	Q3.1	18:46:33.9	+47:51:08	17.10	0.800	e†	B
10784623	J19045+4810	Q4.2	19:04:34.9	+48:10:22	16.95	0.065	d	sdB
10789011	J19136+4808	Q3.2	19:13:36.3	+48:08:24	15.50	0.031	df	sdOB
10961070	J18534+4827	Q4.2	18:53:29.5	+48:27:52	16.99	0.970	d	sdOB
10966623	2M1908+4829	Q3.2	19:08:12.8	+48:29:35	14.87	0.030	bf	B
11337598	J18577+4909	Q3.3	18:57:47.3	+49:09:38	16.11	0.225	d	DA
11350152	J19268+4908	Q3.1	19:26:51.5	+49:08:49	15.49	0.023	d	sdB+F/G
11400959	J19232+4917	Q4.1	19:23:17.2	+49:17:31	16.89	0.577	d	sdB
11558725	J19265+4930	Q3.3	19:26:34.1	+49:30:30	14.95	0.028	f	sdBV
11604781	J19141+4936	Q3.1	19:14:09.0	+49:36:41	16.72	0.006	e†	DA
12021724	J19442+5029	Q4.2	19:44:12.7	+50:29:39	15.59	0.558	e†	sdB
12069500	J19419+5031	Q4.1	19:41:58.6	+50:31:09	13.63	0.654	f	F

Note: The decimal point to the run numbers indicates the relevant month of the mission quarter.
Kp is the magnitude in the *Kepler* bandpass. $F_{\rm cont}$ is the contamination factor from the KIC(zero is no contamination).
The samples are as follows. a: literature, b: 2MASS, c: SDSS, d: *Galex*, e: RPM, f: KIC colour.
†Targets with TNG photometry; ‡described in Fontaine et al. (2011).

subdwarf composites (33 objects), as described in the following section.

One target in the final sample, KIC 10784623, was scheduled for observations but was not observed, as it happens to be located on module 3 which suffered a technical fault early in the fourth quarter (see Section 4) and is no longer in use. Since the spacecraft is rotated every quarter in order to keep its sunshade facing in the right direction, it could be possible to observe it at some time later in the mission.

3 SPECTROSCOPY

All the targets in Table 1 were observed with low-resolution spectrographs at various telescopes, as listed in Table 2. The observations at the Nordic Optical Telescope (NOT) were done with the ALFOSC spectrograph, with grism 6 in 2008 and grism 14 after that. Both gave $R \approx 600$ for the ∼1-arcsec slit we used, and $\lambda = 3300$–6200 Å. On the William Herschel Telescope (WHT), we used the ISIS spectrograph with grating *R*300B on the blue arm ($R \approx 1600$,

Table 2. Log of spectroscopic observations.

Run	Dates	Telescope	P.I., Observer
N1	2008 September 20–21	NOT	JHT, AS
N2	2008 September 22–26	NOT	RO
W1	2009 April 11–12	WHT	CA, RHØ
W2	2009 July 14–16	WHT	CA, TAO
N3	2009 September 7	NOT	JHT, JL
N4	2010 June 9	NOT	JHT, AT
W3	2010 July 2–6	WHT	CA, RHØ
N5	2010 September 27	NOT	JHT, SF, PW

$\lambda = 3100$–5300 Å). Red arm spectra were also obtained, but have not been used for this work. All data were reduced with the standard IRAF procedures for long-slit spectra.

3.1 White dwarfs

There are only five WDs contained in the second half of the survey sample, and all show Balmer-line-dominated spectra typical of DA WDs. One object was initially classified as a DB star in our survey and caused quite some excitement when the *Kepler* light curve was released displaying clear variability with periods resembling a V777 Her pulsator. However, after several efforts to fit the broad helium lines with DB model atmospheres failed, it was realized that the object is actually an AM CVn type of cataclysmic variable, in which helium is accreted on to a WD. This object, KIC 4547333, cannot be analysed with the model spectra used for this paper. A suitable grid of model spectra developed especially for the analysis of this interesting system is described in Fontaine et al. (2011). Since all details of KIC 4547333 are provided in that paper, we will not discuss it further here.

In Table 3, we list the five WDs of the current sample together with the seven DAs and the DB from Paper I. We have attempted to fit model grid spectra to these WDs, using the same procedure as for the sdBs and the grids described in Koester (2010).

One of the five DAs, KIC 11337598, appears to be an unusually rapid rotator (Fig. 1). A rotational velocity of $v \sin i = 1500\,\mathrm{km\,s^{-1}}$ had to be imposed on the model in order to get a reasonable fit. This very substantial velocity corresponds to a rotation period of about 40 s for a typical WD, which is about half of the breakup velocity

Table 3. Spectroscopic properties of the WDs, including eight from Paper I (marked with the † symbol).

KIC	Survey name	$T_{\rm eff}$ (kK)	$\log g$ (dex)	Class	Run
3427482†	J19053+3831	Poor fit		DA	W2
4829241†	J19194+3958	19.4(5)	7.8(3)	DA2	W1
5769827	J18547+4105	66(2)	8.2(3)	DA0	W1
6669882†	J18557+4207	30.5(5)	7.4(3)	DA1	W2
7129927	J19409+4240	Composite DA2+DA3			N3,N5
8682822†	J19173+4452	23.1(5)	8.5(3)	DA2	W1
9139775†	J18577+4532	24.6(5)	8.6(3)	DA2	W2
10198116	J19099+4717	14.2(5)	7.9(3)	DA3	W1
10420021†	J19492+4734	16.2(5)	7.8(3)	DA3	W3
11337598	J18577+4909	22.8(5)	8.6(3)	DA2	N1,W3
11514682†	J19412+4925	32.2(5)	7.5(3)	DA1	W1
11604781	J19141+4936	9.1(5)	8.3(3)	DA5	W2
11822535†	WD J1943+500	36.0(5)	7.9(3)	DA1	N2
6862653†	J19267+4219	Poor fit		DB	W2

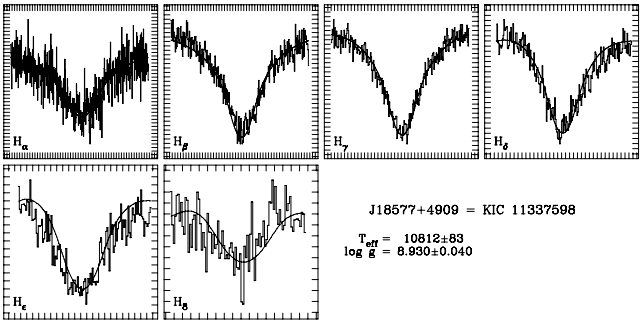

Figure 1. Spectrum and line-profile fit to KIC 11337598, assuming a rotational broadening of $1500\,\mathrm{km\,s^{-1}}$. The spectrum, in particular the higher resolution red-arm part, is rather noisy, but the extraordinary broad cores are clearly evident. The ticks mark 5 Å on the x-axis and 2 per cent of the continuum level on the y-axis. The uncertainties stated in the figure are the formal fitting errors. The real errors are much larger since the radial velocity and $v \sin i$ are not fitted simultaneously.

(higher if seen at a low inclination angle). While the spin period is higher than the *Kepler* SC sampling frequency, if a modulation with this period were present in the light curve, it might still show up in the Fourier transform (FT), as the high sensitivity of *Kepler* photometry would have permitted us to see such high frequencies as reflections across the Nyquist frequency. Although the fit shown in Fig. 1 looks reasonable considering the noise, we cannot completely rule out a weak magnetic field as a possible alternative or contributing effect to the Balmer line broadening. A much higher signal-to-noise ratio (S/N) spectrum would be required to clearly distinguish these possibilities. The *Kepler* light curve shows no high-frequency signal, but does show a low-amplitude long-period peak (see Section 4.3).

In three cases, the spectra do not provide acceptable fits. When fitting KIC 7129927, the solution converges to about $T_{\rm eff} = 23\,000$ K and $\log g = 7.3$, but the cores are clearly not well fitted (Fig. 2). A new spectrum was recently obtained, and it was confirmed that

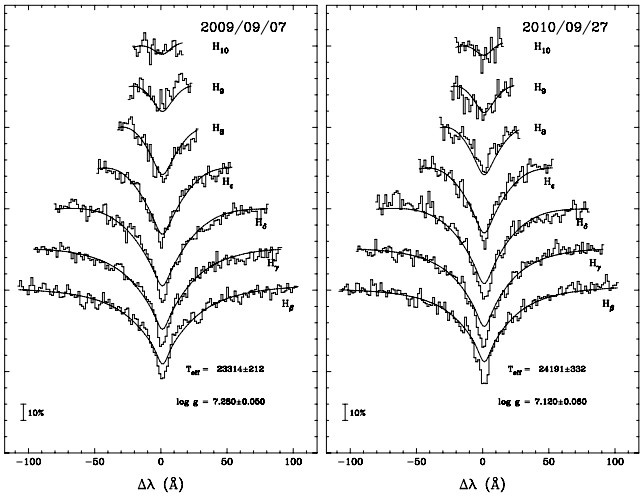

Figure 2. Spectrum and line-profile fit to two observations of KIC 7129927, taken a year apart. Both spectra show that the target has unusually narrow Balmer line cores superimposed on a normal broad DA profile. The uncertainties stated in the figure are the formal fitting errors, but as the fit is obviously far from adequate and the object most likely composite, the best-fitting solution can be quite far from the true parameters of the brightest system component.

the strange features in the cores of the DA2 spectrum were real. We conclude that these features can be explained by a composite DA+DA binary, with the fainter component having somewhat narrower Balmer lines than the hotter component. There may be a small shift between the cores of the broad and narrow components, but this is hard to quantify from the low S/N spectra currently available. The low S/N also prevents a reliable decomposition, so deeper spectroscopy of this object is encouraged.

The two cases marked with 'Poor fit' in Table 3 are of faint targets obtained in bright sky conditions, and the background subtraction appears to be inadequate. The intention when the spectra were made was only to provide a spectroscopic class for all the targets in the sample, and in these cases the quality turned out to be too poor to obtain reliable physical parameters. However, there is no doubt about the classification. The star listed as a DA WD shows the broad and deep Balmer lines typical for DAs not too far from the ZZ Ceti instability strip. The DB is most likely around 16 000 K, much too cool to be a V777 Her pulsator. At $Kp = 18.2$ it is also the faintest star in our sample. As none of these stars show any sign of variability above the 4σ limit, we have not attempted to obtain higher quality spectra.

3.2 Hot subdwarf stars

The majority of the stars constituting the current half of our survey sample are normal sdB or sdOB stars (26 objects), out of which one is clearly composite with an F/G-type companion. Of the remaining subdwarfs, one is a helium-poor sdO star and six are He-rich sdO or sdOB stars. Note that we distinguish between the common He-sdOB stars that show He I and He II lines with almost equal depth, and the hotter and rarer He-sdO stars that show predominantly He II lines. The former are seen in various surveys to form a narrow band at around 40 000 K (e.g. Stroeer et al. 2007), while the latter do not cluster in the $T_{\rm eff}/\log g$ plane (Østensen 2009). As in Paper I, we have fitted the spectra of the sdB and sdOB stars to model grids, in order to determine effective temperature ($T_{\rm eff}$), surface gravity ($\log g$) and photospheric helium abundance ($\log y = \log N_{\rm He}/N_{\rm H}$). The fitting procedure used was the same as that of Edelmann et al. (2003), using the metal-line blanketed local thermodynamic equilibrium (LTE) models of solar composition described in Heber, Reid & Werner (2000). The usual caution about systematic effects, when comparing parameters derived from fitting upon grids created using different methodologies, obviously applies. For the non-pulsators, we list the physical parameters in Table 4 together with the variability limits from the frequency analysis discussed in the next section. The parameters of the pulsators are given in Table 6 later in the text, together with their variability data. For the He-rich subdwarfs and the hot sdO we do not provide physical parameters, as they are beyond the range of our LTE grid.

4 *Kepler* PHOTOMETRY

The *Kepler* photometer operates with an intrinsic exposure cycle consisting of 6.02-s integrations followed by 0.52-s readouts. The SC photometry is a sum of nine such integrations, and LC photometry is a sum of 270 (Gilliland et al. 2010b). The LC cycle produces artefacts in the SC light curve, not just at the LC frequency, $f_{\rm LC} = 566.391\,\mu$Hz, but at all harmonics of this frequency up to the Nyquist frequency, which is $f_{\rm Nyq} = 15 f_{\rm LC} = 0.5 f_{\rm SC} = 8496.356\,\mu$Hz. In most SC light curves, this artefact comb has its strongest peak at $9 f_{\rm LC} = 5098\,\mu$Hz. For details on the *Kepler* data processing pipeline, see Jenkins et al. (2010).

The *Kepler* spacecraft performs a roll every quarter, in order to keep its solar panels and sunshield facing the sun. The mission therefore naturally breaks down into quarterly cycles, and the two quarters of data analysed here are referred to as Q3 and Q4, respectively. Each quarter is then split into monthly thirds, and the collected photometric data are downloaded after each such run. When this happens, the spacecraft must change its attitude to point

Table 4. Properties of the sdB stars with no significant pulsations.

		100–500 μHz			500–2000 μHz			2000–8488 μHz			Spectroscopic data			
KIC	Name	σ (ppm)	A_+ (σ)	f_+ (μHz)	σ (ppm)	A_+ (σ)	f_+ (μHz)	σ (ppm)	A_+ (σ)	f_+ (μHz)	$T_{\rm eff}$ (kK)	$\log g$ (dex)	$\log y$ (dex)	Run
2020175	J19308+3728	30	3.4	482	29	3.5	1345	29	3.7	4432	33.0(9)	5.90(5)	−1.5(1)	N1
2304943	J19275+3738	53	4.8	365	50	3.2	655	51	3.8	2290	31.2(5)	5.82(7)	−1.7(1)	N2
3353239	J19367+3825	20	3.0	497	20	3.3	835	19	3.4	4658	32.4(2)	5.75(5)	−2.7(2)	W1
3527028	J19024+3840	96	2.9	376	93	3.5	1899	94	3.7	3116	30.1(3)	5.58(5)	−2.7(4)	W2
5340370	J18535+4035	96	3.0	107	94	3.3	1832	94	3.5	4244	30.2(2)	5.61(4)	−2.4(1)	W2
5938349	J18521+4115	54	2.9	457	54	3.8	1422	54	4.4	6517	31.9(5)	5.83(6)	−2.6(2)	W1
6522967	J19279+4159	65	3.5	217	63	3.4	1228	63	4.4	8082	34.3(6)	5.27(9)	−2.7(4)	W1
6614501	J19368+4201	28	5.3	365	27	3.4	1179	27	4.1	4381	23.1(4)	5.50(5)	−3.0(1)	W1
7104168	FBS 1907+425	18	3.1	448	18	3.6	732	18	3.8	3557	36.5(5)	5.67(10)	−0.7(1)	N1
7799884	J18456+4335	57	3.1	368	56	4.0	564	56	3.6	7327	31.8(4)	5.68(6)	−2.0(1)	N1
8874184	J19084+4508	50	3.1	316	46	4.1	1813	46	3.8	8361	32.4(9)	5.84(6)	−1.8(1)	N2
9095594	J19369+4526	74	3.3	297	71	3.4	1254	71	3.7	8010	29.3(4)	5.19(6)	−3.0(1)	W1
9211123	J19144+4539	28	3.0	283	27	3.4	1658	26	3.8	2033	34.7(4)	5.11(6)	−2.9(1)	N2
10149211	J19393+4708	22	6.9	370	22	3.4	1434	21	3.6	6124	27.6(4)	5.42(5)	−2.7(1)	W1
10462707	J19144+4737	57	3.6	368	57	3.9	561	57	4.1	8206	28.6(4)	5.25(6)	−3.0(1)	W1
10784623	J19045+4810	Not observed yet									29.4(5)	5.44(8)	−2.9(1)	N2
10789011	J19136+4808	23	3.9	364	22	3.2	1513	22	3.9	6243	34.1(2)	5.69(5)	−1.4(1)	N2
10961070	J18534+4827	108	3.1	421	107	3.7	587	109	4.1	4623	37.4(3)	6.05(5)	−1.0(1)	W2
11350152	J19268+4908	24	3.6	253	20	4.2	630	19	3.6	5958	35.6(3)	5.57(5)	−1.7(1)	N2
11400959	J19232+4917	51	3.4	477	49	3.4	688	49	3.9	5568	39.5(4)	6.12(4)	−2.9(1)	W2
12021724	J19442+5029	30	3.3	436	29	3.5	531	29	3.7	7527	26.2(3)	5.40(4)	−2.3(1)	W1

Notes: σ is the mean of the amplitude spectrum in the region stated. A_+ and f_+ give the amplitude and frequency of the highest peak, respectively.

Table 5. Properties of the non-sdB stars with no significant pulsations.

KIC	Survey name	100–500 μHz σ (ppm)	100–500 μHz A_+ (σ)	100–500 μHz f_+ (μHz)	500–2000 μHz σ (ppm)	500–2000 μHz A_+ (σ)	500–2000 μHz f_+ (μHz)	2000–8488 μHz σ (ppm)	2000–8488 μHz A_+ (σ)	2000–8488 μHz f_+ (μHz)	Spectroscopic classification
2303576	J19263+3738	102	2.9	345	101	3.3	788	100	3.9	2160	He-sdO
3343613	J19272+3827	43	3.9	364	40	3.4	1441	39	3.7	7517	He-sdOB
5769827	J18547+4105	59	3.1	236	56	3.5	577	55	3.6	6507	DA0
6878288	J19436+4220	42	3.6	148	42	3.4	1664	42	3.9	4311	He-sdOB
7129927	J19409+4240	39	3.2	418	38	3.4	960	38	3.9	5495	DA+DA
7335517	J18431+4259	31	3.6	187	33	3.7	801	32	3.9	5533	sdO
8054179	J19569+4350	14	3.4	236	12	3.3	1499	12	3.8	2108	He-sdOB
10198116	J19099+4717	32	5.5	369	31	4.0	1485	31	3.8	5541	DA3
10207025	J19260+4716	40	3.4	107	35	3.3	591	35	4.0	7486	He-sdO
10449976	J18472+4741	15	3.1	459	16	3.3	1200	16	4.1	4569	He-sdOB
11337598	J18577+4909	67	2.9	288	64	3.6	817	64	3.7	7858	DA1 (rot)
11604781	J19141+4936	59	3.1	350	59	3.7	1405	59	3.9	5677	DA5

Note: σ is the mean of the amplitude spectrum in the region stated. A_+ and f_+ give the amplitude and frequency of the highest peak, respectively.

its main antenna at the Earth. During these events, observations cease and the change in pointing causes a thermal transient in the spacecraft and its instrument. Afterwards, the spacecraft takes some days to reach an equilibrium state, and light curves of many targets show deviations, as shifts in the focal plane slightly change the contamination from nearby objects. Similar thermal transients are seen after unforeseen events cause the spacecraft to enter a safe mode and switch off its detector electronics, which then takes some time to warm up after resumption of normal operations. Pointing tweaks also produce discontinuities in faint objects due to changes in the contamination from nearby objects, but during Q3 and Q4 no pointing tweaks were required, leaving fewer corrections necessary than in the earlier quarters. All data sets could be corrected by one or two continuous curves, consisting of a leading exponential decay followed by a polynomial of no more than third order.

Only four events are significant enough to require corrections to the Q3 and Q4 light curves. There is a 1-d gap in Q3.1 data, between MJD 55113.55 and 55114.34, caused by a loss of fine pointing control.[2] *Kepler* entered safe mode at the very end of Q3.2, so the event did not affect these light curves significantly, but Q3.3 light curves are slightly shorter than intended, after the 2 d of downtime, and the first few days of these suffer from a more severe thermal excursion than usual. In Q4.1, on MJD 55205, CCD-module 3 failed. The loss of the module produced temperature drops within the photometer and telescope structure (Van Cleve 2010), and these affect the light curves in a minor way, similar to a pointing tweak. The most significant event happened in the middle of Q4.2, when the spacecraft entered safe mode for 4 full days between MJD 55229.35 and 55233.31, the longest downtime of the first mission year.

4.1 Pulsation limits

In Tables 4 and 5, we list the limits from our Fourier analysis of the *Kepler* light curves where no clear pulsations were found, for the non-sdB and sdB stars, respectively. As in Paper I we provide, for three different frequency ranges, the arithmetic mean (which we consider to be the standard deviation, σ) of the amplitude spectrum in each frequency range and the amplitude (A_+) and frequency (f_+) of the highest peak. A_+ is given as the ratio of the peak amplitude to the σ level. Frequencies associated with binary and other types of long-period variability are discussed in Section 4.3.

As noted in Paper I, peaks with amplitudes as high as 4.1σ are seen in many of the light curves, and we do not consider these to be significant. Frequencies associated with binary and other types of long-period variability are discussed in Section 4.3.

For the binaries with harmonics that have significant amplitudes above 100 μHz, we fitted the main period (and harmonic) with sines as part of the detrending process. The residual light curves were then σ-clipped at 4σ to remove outliers before beginning the Fourier analysis. Only for the relatively high-amplitude binary, KIC 7335517, did this procedure leave any significant residuals. For this case, the A_+ listed in Table 5 ignores the first three harmonics of $f_{\rm orb} = 84.33$ μHz.

For the non-sdB stars, the only marginally significant period (5.5σ) is seen in KIC 10198116, at 369 μHz. However, structure between 360 and 370 μHz is seen in many other stars of a wide range of spectral types and observed in various quarters, and has now been flagged as most likely instrumental in origin.

The limits for the sdB stars that were not found to show clear pulsations are given in Table 4. Here we see three stars that show significant peaks between 364 and 372 μHz, which we consider to be spurious. Excluding this frequency range would drop A_+ for the low-frequency range to below 3.3σ for all three stars. Two stars show peaks at 4.4σ in the high-frequency domain, but these peaks are too low to be significant if the light curve is split into halves, and we therefore consider the evidence of pulsations in these stars to be too weak to claim detection. None of the stars show any other peaks higher than 4σ in the high-frequency region, either in the full light curve or in the individual halves.

As mentioned above, the LC artefacts introduced at $nf_{\rm LC}$ up to the Nyquist frequency make us effectively blind to pulsators with periods at these frequencies. However, due to the 30-d length of the runs, the resolution is sufficiently high that these blind spots are quite insignificant. A second cause of concern is the Nyquist limit itself, which at 120 s represents a period typically seen in sdB stars. Of the 49 sdBV stars listed in Østensen et al. (2010c), 13 have periods at or shorter than 120 s. The shortest period reported to date is 78 s in EC 01541–1409 (Kilkenny et al. 2009). The sdO pulsator, J16007+0748 (Woudt et al. 2006), is a particular case of concern since all the 13 periods detected in this star lie between 57 and 119 s (Rodríguez-López et al. 2010). However, periods shorter than the

[2] The times used here are modified Julian dates (MJD = JD – 250 0000.5).

Table 6. Properties of the sdBV stars.

		Kepler data					Spectroscopic data			
KIC	Name	σ (ppm)	N_f	$f_{\rm med}$ (μHz)	$f_{\rm min}$ (μHz)	$f_{\rm max}$ (μHz)	$T_{\rm eff}$ (kK)	log g (dex)	log y (dex)	Run
7668647	FBS 1903+432	22	15	173.3	115.9	345.8	27.7(3)	5.45(4)	−2.5(1)	N1
8302197	J19310+4413	41	6	183.3	126.3	305.8	26.4(3)	5.32(4)	−2.7(1)	W2
10001893	J19095+4659	23	24	262.9	77.5	391.4	26.7(3)	5.30(4)	−2.9(1)	N2
10553698	J19531+4743	19	30	228.1	104.3	492.9	27.6(4)	5.33(5)	−2.9(2)	W1
11558725	J19265+4930	17	36	260.5	78.2	390.9	27.4(2)	5.37(3)	−2.8(1)	W1

Nyquist limit are still detectable, with a smearing penalty factor given by $\sin(x)/x$, where $x = \pi f \Delta t_{\rm exp}$ (Kawaler et al. 1994). The smearing drives all amplitudes to zero as the sampling frequency is approached, but for most frequencies between $f_{\rm Nyq}$ and the sampling frequency the recovered amplitudes are still significant. For *Kepler*, we should recover 30 per cent of the amplitude for pulsation periods of 80 s. The corresponding frequencies will appear in the FT reflected around $f_{\rm Nyq}$, as was seen for the first harmonic of the main pulsation mode in KIC 10139564 (Paper II).

4.2 New pulsators

Five clear V1093 Her pulsators were detected in the second half of the survey phase (Table 6). The noise level (σ) was measured in the region 1000–2500 μHz. In addition to the number of significant pulsation modes detected in the *Kepler* photometry (N_f), and the minimum and maximum pulsation frequencies, we also provide the power-weighted mean frequency, $f_{\rm med}$. The spectroscopic parameters as determined from our fits are also listed, and all stars are seen to cluster at the hot end of the g-mode region between 26 000 and 28 000 K.

Of the five V1093 Her pulsators described in Paper III, three were found to show low-amplitude short-period pulsations in the frequency range typical for V361 Hya stars. Recently, Charpinet et al. (2011) have concluded that the single short-period peak found in KIC 2697388 is consistent with a predicted p mode in their model that fits the observed g-mode spectrum, thereby making the case that these objects represent a new kind of hybrid sdBV.

In the current sample, KIC 7668647 shows two peaks at 4738 and 4739 μHz, at around 5σ. The peaks are most significant in the first half of the run and drop below the 4σ limit in the second half of the run. KIC 8302197 shows no significant peaks (higher than 4.1σ) in the short-period pulsation range. KIC 10001893 shows a single 5.7σ peak at 2925.8 μHz. KIC 10553698 shows a pair of 4.5σ peaks at 3073 μHzand also some structure at 4070 μHz. KIC 11558725 also shows peaks at 3073 μHz, the highest at 8.7σ. It is suspicious that two stars show the same frequency, but the former was observed in Q4.1 and the latter in Q3.3. Thus, it is not obvious that these are artefacts, and none of the frequencies found in these stars has been associated with artefacts before. Thus, it appears that four of the five long-period pulsators might be hybrid pulsators, but the amplitudes are low so the hybrid nature needs to be confirmed. See Paper VII for more details.

Fig. 3 is identical to fig. 3 in Paper I, but with the new pulsators and non-pulsators added. Unlike in the first half of the sample, we here clearly have non-pulsators at $T_{\rm eff}$ lower than the transition region between the p- and g-mode pulsators (at ∼28 000 K).

KIC 6614501 at $T_{\rm eff} = 23\,100$ K is unusual as it lies well below the extreme horizontal branch (EHB) in Fig. 3. It also shows a light-curve signature that we interpret as binary, as discussed in Section 4.3. This could indicate that this sdB is another example of the rare post-red giant branch (RGB) WD progenitors that are evolving directly from an RGB evolution interrupted by a common-envelope

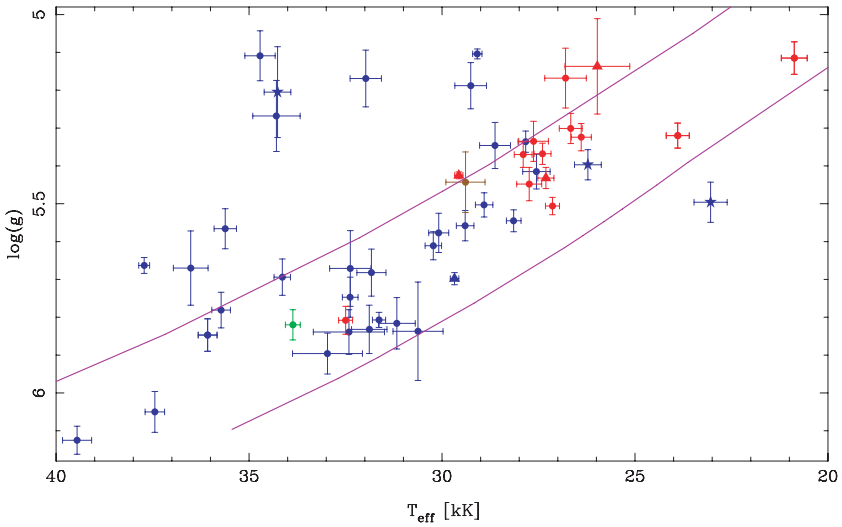

Figure 3. The $T_{\rm eff}/\log g$ plane for the sdB stars in our sample. Red symbols indicate the pulsators, blue symbols the non-pulsators, with the transient pulsator of Paper I marked with a green bullet and the as-yet unobserved sdB with a brown symbol. The apparently single sdBs are marked with bullets, the sdB+dM reflection binaries with triangles and the sdB+WDs with stars. The curves indicate the approximate location of the zero-age and terminal-age EHB for a canonical sdB model.

ejection and towards the WD cooling curve, such as HD 188112 (Heber et al. 2003). Unlike the EHB stars, for which the core managed to reach sufficient mass for helium ignition before the envelope was ejected, these stars are much less massive and will become low-mass He-core WDs. The current temperature and gravity of KIC 6614501 are consistent with the evolutionary tracks of Driebe et al. (1999) for a mass of the primary of $\sim$0.24 $M_{\odot}$. Its FT does show some weak peaks around 365 μHz, but as mentioned earlier, these are most likely artefacts.

KIC 12021724 is located at 26 200 K and has absolutely no significant peaks in the FT above 35 μHz. However, like KIC 6614501, it shows a likely binary period.

4.3 Binaries and other long-period variables

In Table 7, we list the 14 binaries and other long-period variables that we have detected in the current half of the sample. The periods range from 3.3 h to almost 5 d, and the peak-to-peak amplitudes range from a few per cent to a few hundred ppm.

The sdO star KIC 7335517 is the clearest binary candidate, with the maxima slightly sharper than the minima (Fig. 4, upper left panel), as is typical for the temperature effects that are seen when a hot subdwarf irradiates one hemisphere of a cool companion. The folded light curve is similar to that of KBS 13, observed in Q1, and the semi-amplitude is about the same. We judge the temperature of the primary to be above 40 000 K, so the reflection effect should be much higher than what is seen, if the system is seen at high inclination. Thus, the system is most likely seen at low inclination, as for KBS 13, or else the companion is substellar.

The remaining nine objects shown in Fig. 4 all display very low-level photometric modulations that may be due to orbital effects, but we do not consider any of these as being likely to have M-dwarf companions. A more likely companion would be a WD, in which case the light curve should display a combination of ellipsoidal deformation and Doppler beaming, such as seen for KPD 1946+4340 (Bloemen et al. 2011). In particular, KIC 6614501 has the double-peaked structure, with alternating maxima and minima of roughly equal depth, that characterizes such beaming binaries. Splitting the light curve into halves reveals a consistent shape, as expected for an orbital effect. KIC 10462707 and 12021724 are also likely to be sdB+WD binaries, and a WD companion is a possible interpretation for the He-sdO KIC 2303576 as well.

Table 7. Binaries and other long-period variables.

KIC	Period (d)	Amp. (per cent)	Class	Main variability
2303576	0.192 06	0.8	He-sdO+?[a]	Bin/cont
3527028	2.105 40	0.5	sdB+?	Unknown
5340370	0.20–0.72	–	sdB+?	Unknown
6614501	0.157 46	0.12	sdB+WD?	Binary
6878288	3.040 65	1.0	He-sdOB+?	Unknown
8874184	2.636 70	0.8	sdB+?	Var. comp
7335517	0.137 25	6.0	sdO+dM	Reflection
8054179	–	0.02	He-sdOB	Aperiodic
10149211	0.605 13	0.5	sdB+?	Var. comp
10462707	0.788 80	0.08	sdB+WD?	Binary
11337598	0.093 26	0.04	DA1 (rot)	Spin period?
11350152	3.3	1.5	sdB+F/G	Var. comp
11604781	4.879 88	0.5	DA5	Unknown
12021724	0.674 90	0.07	sdB+WD?	Binary

[a]? signifies an uncertain or an undeterminable classification.

KIC 6878288, 11604781 and 3527028 all show monoperiodic light-curve variations that range between 2 and 5 d and do not change between the first and second halves of the run. The He-sdOB KIC 6878288 and the regular sdB KIC 3527028 are unlikely to show such long periods intrinsically. But both have contamination factors, $F_{\rm cont}$, indicating that around half the light comes from other sources near the intended target. This makes it rather futile to speculate about whether the modulation comes from the subdwarfs, close companions or nearby objects. KIC 11604781 is the only regular WD star in the current sample that shows any long-period modulations. With $F_{\rm cont} = 0.006$, any reasonable effect from a contaminating object is effectively ruled out. The spectrum is also void of any features indicating a cool companion, even in the region around Hα. For such a cool DA, the companion would have to be substellar not to contribute to the optical spectrum. There are no features in our classification spectrum that can offer clues to the origin of the photometric variability, such as trace of a companion or a magnetic field, so we have at present no theory that could explain the 4.88-d signal.

KIC 10149211 and 8874184 show variations with a main period and a strong first harmonic, and small but significant changes in the shape of the modulation between the first and the second halves. Such variations are unlikely to originate from the hot subdwarf star itself, and with $F_{\rm cont}$ between 9 and 24 per cent they are most likely from a contaminating object. A possible interpretation is that the contaminating star is heavily spotted and has more spots on one hemisphere than on the other (see e.g. Siwak et al. 2010).

The FT of KIC 11350152 is dominated by a strong 3.16-d period and its first harmonic. There are no other significant peaks in the FT. As shown in Fig. 5, there are substantial variations from cycle to cycle. Also here the most likely interpretation is that the main period seen is the rotation period of a spotted companion, but a pulsating companion cannot be ruled out. Our blue spectrum shows clear signatures of an F–G companion, with K and H lines too broad to be interstellar, and a clear *g* band. The 2MASS infrared (IR) photometry indicates a rising IR flux, and the object appears single in images, so the cool star is likely to be the accretor responsible for stripping the envelope off the sdB progenitor when it is on the RGB. Also, $F_{\rm cont}$ is insignificant so the variations cannot be ascribed to any nearby objects.

KIC 5340370 shows unusual behaviour below 100 μHz. The periods appear to change completely between the first half of the run and the second, so we have computed a wavelet transform (WFT) rather than the regular FT, using the WWZ algorithm of Foster (1996). The WFT is shown in Fig. 6, and in the first half two clear peaks are found at 0.55 and 0.73 d (16 and 20 μHz). These peaks are no longer detectable in the second half but have been replaced by broad features in the region between 0.2 and 0.4 d ($\sim$30 and 60 μHz).

KIC 8054179 shows a light curve with considerable power in the FT at frequencies below 100 μHz, but no clear peaks. The amplitude of the variability is only at the 200-ppm level and can easily be caused by a contaminating star. However, it is interesting to note that in the first half of the survey, we also saw aperiodic variability in another He-sdOB star, KIC 9408967, but then at a somewhat higher amplitude than here.

The WD which we suspected to be an extremely rapid rotator in Section 3.1, i.e. KIC 11337598, shows no significant peaks in the FT, except for a single low-amplitude peak at 124 μHz(= 0.093 d). With an amplitude of only 360 ppm, this is far too low to be a binary signal for such a short period orbit, unless the system is seen improbably close to pole-on. If the 0.093-d period is instead the spin period

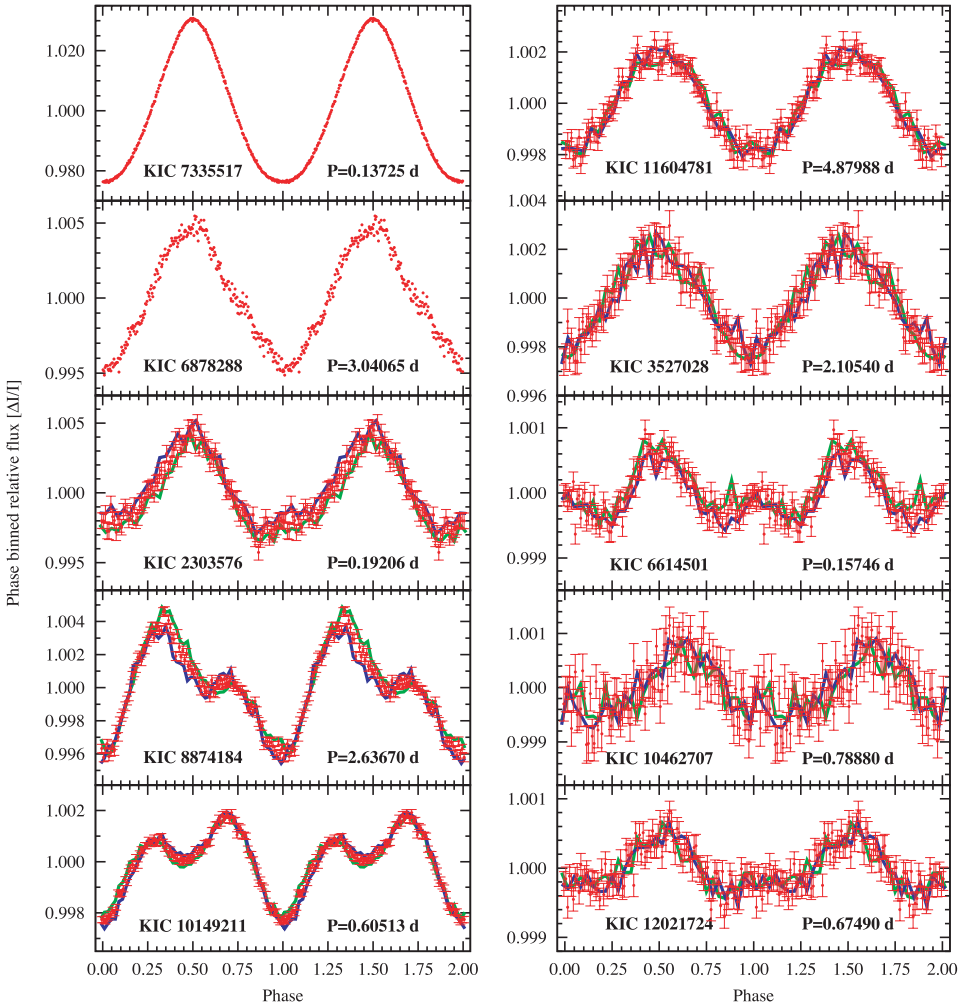

Figure 4. Data of 10 binary candidates folded on the main period. The light curves are folded on the periods given in Table 7 and are repeated in each panel. For the first two we use 250 bins, and the data are plotted as points. For the rest we use either 100 bins or 30 bins, due to the lower signal, and the error bars shown are the rms values for the points in each bin. We also subdivided the eight last observation runs into two halves and folded these separately. The resulting curves are shown as continuous green and blue lines. Two cycles are shown for clarity.

of the WD, then the spectroscopic broadening cannot be caused by rotation. A possible explanation could involve a relatively weak magnetic field causing Zeeman splitting of the Balmer lines, being sufficiently strong to produce the observed broadening without producing resolved splitting at our low S/N. The 0.093-d photometric period could then be the spin period of the WD, made visible by weak spots on the surface of the WD, as observed in WD 1953–011 (Brinkworth et al. 2005). A similar period of 0.0803 d was observed in GD 356, although at 10 times the amplitude, and interpreted in a similar way by Brinkworth et al. (2004). With $F_{\rm cont} = 0.225$ the signal can also be from a contaminating object, so no firm conclusions can be made. But better spectroscopy could easily be invoked to detect any Zeeman splitting of the Balmer lines or confirm our original hypothesis of rapid rotation. In either case, KIC 11337598 is an intriguing WD.

5 DISCUSSION AND CONCLUSIONS

We have completed a survey for compact pulsators with *Kepler*, and as far as the sdB stars are concerned the survey has been a great success. Unfortunately, no pulsating WDs were found in the survey sample. This is not entirely surprising as the number of DA WDs surveyed is only 13, and of these only a couple are anywhere close to the ZZ Ceti instability strip. One star that sits slightly above the instability region is KIC 10420021, observed in Q2.2. As we noted in Paper I, it does have a 4.5σ peak in the FT at 196.4 μHz. It was re-observed for 3 months in Q5, but a quick analysis of this recently released light curve reveals no trace of any significant signals at periods shorter than a few days.

The spectroscopic survey used to describe the targets in Paper I and in this paper was conducted mostly after the deadline for submitting targets for the *Kepler* survey phase had passed. If such a survey had been made earlier, it would have been evident that the WD sample was too small to have a significant chance of containing WD pulsators. But if more stars fainter than $Kp = 17.5$ had been retained in the sample, the chance of finding WD pulsators would have been much higher, since at such faint magnitudes hot subdwarfs will have to be located beyond the Galactic disc, and no longer dominate UV-selected samples. As we have seen from the few stars in our sample that have magnitudes close to $Kp = 18$, the *Kepler* photometry is still excellent with 4σ detection limits around the millimagnitude level, even after taking into account substantial contamination factors.

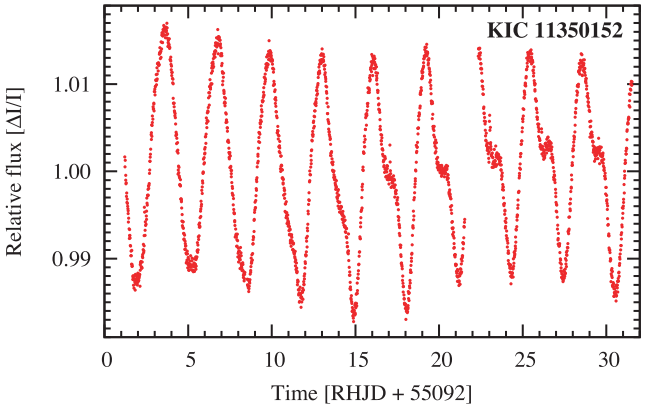

Figure 5. The light curve of KIC 11350152 is dominated by a period of 3.16 d, but the shape of the light curve is changing from cycle to cycle. The light curve was binned so that each point represents 20 SC exposures, in order to reduce the noise.

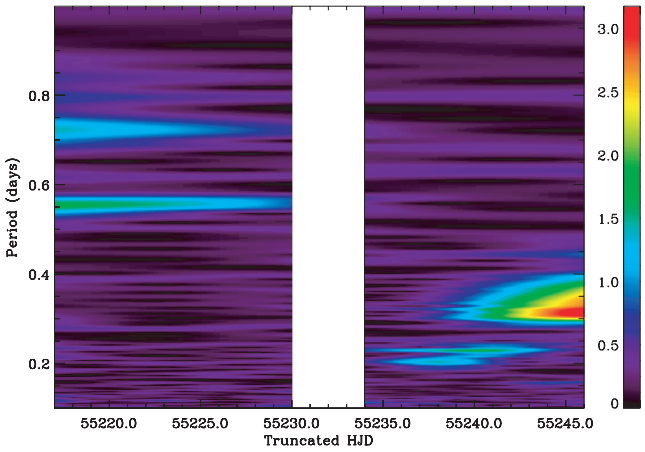

Figure 6. The WFT of KIC 5340370 shows clear periodicities at about 0.55 and 0.72 d in the first part of the light curve. These apparently disappear completely and are replaced briefly by peaks at 0.2 and 0.23 d, which are quickly replaced by a strong and broad structure between 0.31 and 0.39 d. The gap corresponds to the 4-d safing event in Q4.2.

The fact that the survey did not reveal any sdO pulsators was not a surprise, since only one such object has been revealed to date, implying that these objects are exceedingly rare. Of the two objects in the survey classified as sdO+F/G binaries, similar to the prototype J16007+0748 (Woudt et al. 2006), one (KIC 9822180) did show a marginal peak and will be re-observed for 3 months in Q6. In the current half of the sample only one sdO star is not helium rich, and this object, KIC 7335517, is the clearest photometric binary in the sample. This object is most likely much cooler than J16007+0748 and more similar to the eclipsing sdO+dM binary AA Dor, but seen at a low inclination angle.

During the first year of the *Kepler* mission, we have surveyed 32 sdB pulsator candidates hotter than 28 000 K and found only one clear and unambiguous V361 Hya pulsator (Paper II). One other sdB star shows a single significant short-period frequency that drops systematically in amplitude until it is below the detection limit (Paper I). A third pulsator, 2M1938+4603, was found in an eclipsing binary and shows an exceptionally rich pulsation spectrum, which includes short, long and intermediate periods. However, it has no strong (above 500 ppm) pulsation modes, which thus make it quite an exceptional hybrid pulsator. All these stars were discovered in the first half of the survey sample, and the current sample of 17 stars above 28 000 K contains no further V361 Hya pulsators. This means that the number of short-period pulsators found in the *Kepler* sample is actually less than the 10 per cent fraction that has been found in ground-based surveys (Østensen et al. 2010c), at least when considering the fact that 2M1938+4603 would have been almost impossible to recognize as a pulsator from the ground.

For the V1093 Her pulsators, in the first half of the survey we found only one star below 28 000 K that was not pulsating and that one was less than 1σ below this temperature limit. This led us to the preliminary conclusion that all sdBs below 28 000 K may be pulsators. However, in the current sample we find that only five out of eight stars below 28 000 K are pulsators. Only one of these are within 1σ of the temperature boundary. The remaining two appear to be sdB+WD short-period binaries, judging from the long-period variations in their light curves. These are also the only two short-period sdB+WD binaries we have been able to identify in the current sample. We do not see any reason why pulsations should be systematically suppressed in sdB+WD binaries. After all, the well-studied V361 Hya star KL UMa is known to be in a $P = 0.376$ d binary with a WD companion (O'Toole, Heber & Benjamin 2004) and V2214 Cyg in a $P = 0.095$ d binary (Geier et al. 2007). However, as pointed out by Østensen (2009), KL UMa is the only well-studied sdBV of those known to be located in the boundary region between the V361 Hya and the V1093 Her pulsators for which hybrid pulsations have not been detected. One may speculate that g modes can be suppressed somehow in sdB+WD binaries, but this is not the case. Of the nine V1093 Her stars described in the literature, three have been published as sdB+WD binaries: HZ Cnc ($P = 27.81$ d; Morales-Rueda et al. 2003), V2579 Oph ($P = 0.83$ d; For et al. 2006) and PG 0101+039 ($P = 0.57$ d; Geier et al. 2008). However, in the case of KIC 6614501, its position below the canonical EHB is unexpected for an sdB that has evolved through common-envelope ejection. The absence of pulsations in this star can therefore be explained if it is a low-mass post-RGB star that has not ignited helium in its core rather than a regular EHB star, as such stars would evolve too rapidly to build up a Z bump that can drive pulsations.

The total fraction of pulsators below 28 000 K ended up to be 12 out of 16, or 75 per cent, the same number as the rough estimate given by Green et al. (2003). We are still puzzled by the large fraction of sdB stars that show no trace of pulsations in spite of the unprecedented duration and low noise level provided by *Kepler*. We had expected that the fraction of pulsators would increase with increasing precision, but evidently this has not happened.

Thanks to the exceptional precision of the *Kepler* measurements, we can now conclude that there certainly are sdB stars, both on the hot and on the cold ends of the EHB, that show no trace of pulsations. Possible explanations for the non-pulsators would have to answer why the pulsation driving mechanism is suppressed in some EHB stars and not in others. They may represent a low-metallicity population that either started out being low in iron-group elements or evolved to have low metallicity envelopes, as may be the case in merger models. Time-dependent changes in the iron profiles as discussed by Fontaine et al. (2006a,b) can also explain non-pulsators. They may be the youngest among the EHB population, for which an iron opacity bump in the driving region has yet to accumulate, or they can be the oldest EHB stars for which low-level winds have depleted the iron reservoir.

Another significant result of our survey is that many of the V1093 Her pulsators show signs of hybrid behaviour, with single low-amplitude modes in the high-frequency region. The V361 Hya pulsator we found also displays a single mode in the long-period

region. This indicates that hybrid behaviour is not unusual for sdBV stars regardless of their position on the EHB, and not confined to the DW Lyn stars that sit on the boundary between the short- and long-period pulsators in the $T_{\rm eff}/\log g$ plane. With *Kepler* targeting these pulsators at regular intervals throughout its mission, we will soon know if these low-level hybrid modes are transient or persistent features of the pulsation spectra of these stars.

ACKNOWLEDGMENTS

The authors gratefully acknowledge the *Kepler* team and all who have contributed to enabling the mission. Funding for the *Kepler* mission is provided by NASA's Science Mission Directorate.

The research leading to these results has received funding from the European Research Council under the European Community's Seventh Framework Programme (FP7/2007–2013)/ERC grant agreement no 227224 (PROSPERITY), as well as from the Research Council of K.U. Leuven grant agreement GOA/2008/04. ASB gratefully appreciates funding from the Polish Ministry of Science and Higher Education under project no 554/MOB/2009/0. SC thanks the Programme National de Physique Stellaire (PNPS, CNRS/INSU, France) for financial support. ACQ is supported by the Missouri Space Grant funded by NASA.

For the spectroscopic observations presented here we acknowledge the NOT at the Observatorio del Roque de los Muchachos (ORM) on La Palma, operated jointly by Denmark, Finland, Iceland, Norway and Sweden, and the William Herschel Telescope and Isaac Newton Telescope also at ORM, operated by the Isaac Newton Group.

REFERENCES

Abrahamian H. V., Lipovetski V. A., Mickaelian A. M., Stepanian J. A., 1990, Astrofizika, 33, 213
Baran A. et al., 2011, MNRAS, in press (doi:10.1111/j.1365-2966.2011.18486.x) (Paper VII, this issue)
Bloemen S. et al., 2011, MNRAS, 410, 1787
Borucki W. J. et al., 2010, Sci, 327, 977
Brinkworth C. S., Burleigh M. R., Wynn G. A., Marsh T. R., 2004, MNRAS, 348, L33
Brinkworth C. S., Marsh T. R., Morales-Rueda L., Maxted P. F. L., Burleigh M. R., Good S. A., 2005, MNRAS, 357, 333
Charpinet S. et al., 2011, A&A, accepted
Driebe T., Blöcker T., Schönberner D., Herwig F., 1999, A&A, 350, 89
Edelmann H., Heber U., Hagen H.-J., Lemke M., Dreizler S., Napiwotzki R., Engels D., 2003, A&A, 400, 939
Fontaine G. et al., 2011, ApJ, 726, 92
Fontane G., Green E. M., Chayer P., Brassard P., Charpinet S., Randall S. K., 2006a, Baltic Astron., 15, 211
Fontane G., Brassard P., Charpinet S., Chayer P., 2006b, Mem. Soc. Astron. Ital., 77, 49
For B. et al., 2006, ApJ, 642, 1117
Foster G., 1996, AJ, 112, 1709
Geier S., Nesslinger S., Heber U., Przybilla N., Napiwotzki R., Kudritzki R.-P., 2007, A&A, 464, 299
Geier S., Nesslinger S., Heber U., Randall S. K., Edelmann H., Green E. M., 2008, A&A, 477, L13
Gilliland R. L. et al., 2010a, PASP, 122, 131
Gilliland R. L. et al., 2010b, ApJ, 713, L160
Green E. M. et al., 2003, ApJ, 583, L31
Heber U., Reid I. N., Werner K., 2000, A&A, 363, 198
Heber U., Edelmann H., Lisker T., Napiwotzki R., 2003, A&A, 411, L477
Jenkins J. M. et al., 2010, ApJ, 713, L87
Kawaler S. D., Bond H. E., Sherbert L. E., Watson T. K., 1994, AJ, 107, 298
Kawaler S. D. et al., 2010a, MNRAS, 409, 1487 (Paper II)
Kawaler S. D. et al., 2010b, MNRAS, 409, 1509 (Paper V)
Kilkenny D., O'Donoghue D., Crause L., Engelbrecht C., Hambly N., MacGillivray H., 2009, MNRAS, 396, 548
Koester D., 2010, Mem. Soc. Astron. Ital., 81, 921
Martin D. C. et al., 2005, ApJ, 619, L1
Morales-Rueda L., Maxted P. F. L., Marsh T. R., North R. C., Heber U., 2003, MNRAS, 338, 752
Østensen R. H., 2009, Comm. Asteroseismol., 159, 75
Østensen R. H. et al., 2010a, MNRAS, 408, L51
Østensen R. H. et al., 2010b, MNRAS, 409, 1470 (Paper I)
Østensen R. H. et al., 2010c, A&A, 513, A6
O'Toole S. J., Heber U., Benjamin R. A., 2004, A&A, 422, 1053
Prsa A. et al., 2011, AJ, 141, 83
Reed M. et al., 2010, MNRAS, 409, 1496 (Paper III)
Reed M. D. et al., 2011, MNRAS, in press (doi:10.1111/j.1365-2966.2011.18532.x) (Paper VIII, this issue)
Rodríguez-López C. et al., 2010, MNRAS, 401, 23
Siwak M., Rucinski S. M., Matthews J. M., Kuschnig R., Guenther D. B., Moffat A. F. J., Sasselov D., Weiss W. W., 2010, MNRAS, 408, 314
Stoughton C. et al., 2002, AJ, 123, 485
Stroeer A., Heber U., Lisker T., Napiwotzki R., Dreizler S., Christlieb N., Reimers D., 2007, A&A, 462, 269
Van Cleve J. E., 2010, Kepler Data Release Notes 6, http://archive.stsci.edu/kepler/release_notes/release_notes6/Data_Release_06_Notes_2010072313.pdf
Van Grootel V. et al., 2010, ApJ, 718, L97 (Paper IV)
Woudt P. A. et al., 2006, MNRAS, 371, 1497
Yanny B. et al., 2009, AJ, 137, 4377

This paper has been typeset from a TEX/LATEX file prepared by the author.